Human Molecular Genetics, 2013, Vol. 22, No. 12 **2376–2386**
doi:10.1093/hmg/ddt082
Advance Access published on February 19, 2013

Tardbpl splicing rescues motor neuron and axonal development in a mutant *tardbp* zebrafish

Channa A.A. Hewamadduma[1,2], Andrew J. Grierson[1,2], Taylur P. Ma[3], Luyuan Pan[3], Cecilia B. Moens[3], Philip W. Ingham[2], Tennore Ramesh[1,2,†] and Pamela J. Shaw[1,2,*,†]

[1]Department of Neuroscience, Sheffield Institute for Translational Neuroscience, University of Sheffield, 385A, Glossop Road, Sheffield S10 2HQ, UK, [2]MRC Centre for Developmental and Biomedical Genetics (CDBG), Firth Court, University of Sheffield, Sheffield S10 2TN, UK and [3]HHMI and Division of Basic Science, Fred Hutchinson Cancer Research Center, Seattle, WA, USA

Received January 16, 2013; Revised and Accepted February 15, 2013

Mutations in the transactive response DNA binding protein-43 (*TARDBP/TDP-43)* gene, which regulates transcription and splicing, causes a familial form of amyotrophic lateral sclerosis (ALS). Here, we characterize and report the first *tardbp* mutation in zebrafish, which introduces a premature stop codon (Y220X), eliminating expression of the Tardbp protein. Another *TARDBP* ortholog, *tardbpl*, in zebrafish is shown to encode a Tardbp-like protein which is truncated compared with Tardbp itself and lacks part of the C-terminal glycine-rich domain (GRD). Here, we show that *tardbp* mutation leads to the generation of a novel *tardbpl* splice form (*tardbpl-FL*) capable of making a full-length Tardbp protein (Tardbpl-FL), which compensates for the loss of Tardbp. This finding provides a novel *in vivo* model to study TDP-43-mediated splicing regulation. Additionally, we show that elimination of both zebrafish *TARDBP* orthologs results in a severe motor phenotype with shortened motor axons, locomotion defects and death at around 10 days post fertilization. The Tardbp/Tardbpl knockout model generated in this study provides an excellent *in vivo* system to study the role of the functional loss of Tardbp and its involvement in ALS pathogenesis.

INTRODUCTION

Amyotrophic lateral sclerosis (ALS) is a neurodegenerative condition in which death of motor neurons results in progressive failure of the neuromuscular system and death, usually within 2 to 3 years of symptom onset. About 5–10% of ALS cases are familial (fALS) and usually of autosomal dominant inheritance, while 90–95% are sporadic in origin (sALS) (1). Mutations in the transactive response DNA-binding protein-43 (*TARDBP/TDP-43)* gene, (ALS10), that encodes a 43 kDa protein TDP-43, account for ~1% of sALS and 3% of fALS cases (2). TDP-43 is a major constituent of the neurocytoplasmic inclusions (NCIs) present in pathologically affected regions of ALS and frontotemporal lobar degeneration (FTLD) cases (3). The discovery of ~38 mutations in *TARDBP* associated with ALS and FTLD has established the importance of this gene in neurodegeneration (4). It is still debated whether the pathophysiological mechanism related to TDP-43-associated ALS is due to the loss of the normal nuclear function or a toxic gain of cytoplasmic function of TDP-43, or both. Although several *in vivo* and *in vitro* studies have attempted to model the effects of *TARDBP* mutations, the function and regulation of TDP-43 and the pathological consequences of mutant TDP-43 (mTDP-43) remain incompletely characterized (5).

TDP-43 is a predominantly nuclear protein, with several RNA processing functions including roles in the regulation of transcription, alternative splicing, translation and micro RNA biogenesis (6,7). Mislocalization of TDP-43 to the cytoplasm could result in a loss of its normal RNA processing roles in the nucleus (8). *Drosophila* partially lacking TDP-43 are reported viable and have normal morphology, but exhibit

*To whom correspondence should be addressed at: Academic Neurology Unit, Sheffield Institute for Translational Neuroscience, University of Sheffield, 385A, Glossop Road, Sheffield S10 2HQ, UK. Tel: +44 1142222230; Fax: +44 1142222290; Email: pamela.shaw@sheffield.ac.uk
†T. R. and P. J. S. contributed equally.

abnormal locomotive behavior and defective neuromuscular junctions (9). Complete knockdown, however, results in lethality at the second instar stage (10,11). Furthermore, knockout of *Tardbp* in mice causes early lethality around the blastocyst implantation stage of embryogenesis (12,13), complicating analysis of its role in vertebrate neural development and function.

Zebrafish have several key advantages as a vertebrate model organism. Their external development and optical transparency allow high-resolution imaging of all developmental stages and their high fecundity and relatively low maintenance costs facilitate genetic manipulation and high-throughput pharmacological screening for disease modifying agents (14). Several neurodegenerative diseases have been modeled in the zebrafish, although most of these models do not mimic the late-onset neurodegeneration phenotype seen in humans (15). However, the recent development of a zebrafish mutant *sod1* model of ALS mimics several aspects of the adult onset neurodegenerative disease observed in humans and transgenic murine models (16).

Two zebrafish orthologs of *TARDBP*, *tardbp* (chromosome 6) and *tardbp-like* (*tardbpl*)(chromosome 23), have been described. In contrast to *tardbp*, zebrafish *tardbpl* is predicted to encode a truncated protein Tardbpl (303 amino acids), lacking most of the C-terminal region of the corresponding full-length 412 amino acid protein encoded by *tardbp*.

Transient over-expression of mutant tardbp and morpholino-mediated knockdown of tardbp have been recently performed in zebrafish (17,18). A report by Kabashi *et al.* showed that while transient translation knockdown using an antisense morpholino oligonucleotide (AMO) of *tardbp* produced shortening and disorganization of motor neuron axons and reduced coiling ability (18), knockdown of tardbpl produced no obvious defects. The inherent limitations of the AMO technique such as its transient effects, as well as the potential for off-target interactions (19), preclude a full understanding of the role of Tardbp in adult onset neurodegeneration.

We therefore aimed to generate a stable Tardbp deficiency model by TILLING (Targeted Induced Local Lesions in Genome). We identified a *tardbp* null mutant allele with a base substitution that generates a premature stop codon. Analysis of this mutant reveals that a loss of the Tardbp protein results in the upregulation of a novel transcript (*tardbpl-FL*) from the *tardbpl* gene locus by alternative splicing. We further demonstrate that this full-length *tardbpl-FL* transcript can compensate for the loss of Tardbp.

The *tardbp/tardbpl-FL* double knockout zebrafish that we have generated provides a new model to study mechanisms of splicing regulation by Tardbp and of motor neuron injury caused by loss of function of TDP-43. This new zebrafish model may also be valuable in identifying targets for therapeutic manipulation.

RESULTS

Zebrafish homozygous for a *tardbp* null mutation are adult viable

Using TILLING, we identified an ENU-induced allele of *tardbp* (*tardbp*^{fh301}) that has a single nucleotide change c.660C>T resulting in a premature stop codon (TAC → TAA), p.Y220X (Fig. 1A) which truncates the 413 amino acids protein midway through its second RNA binding domain (Fig. 1B). Protein parameter prediction software (http://web.expasy.org/cgi-bin/protparam/protparam) predicts a molecular weight of the premature truncated protein at ∼24 kDa and also predicts it to be unstable (instability index 50.83). The mutation also causes a loss of a CViQI restriction enzyme site, which facilitates genotyping (Fig. 1C). Heterozygous *tardbp*$^{fh301/+}$animals were indistinguishable from their wild-type (WT) siblings. After repeated out-crossing, (F6) *tardbp*$^{fh301/+}$ heterozygotes were selected and in-crossed to generate homozygous *tardbp* mutants (*tardbp*$^{fh301/fh301}$). Interestingly, the expected Mendelian ratios for a heterozygous (*tardbp*$^{fh301/+}$) in-cross were observed at 3 months, indicating that the homozygous (*tardbp*$^{fh301/fh301}$) fish survived at the same rate as the *tardbp*$^{+/+}$ and *tardbp*$^{fh301/+}$ siblings. The mean weights and standard length (Fig. 1D) of each adult F5 zebrafish were recorded at the time of fin clipping for genotyping. *tardbp*$^{fh301/fh301}$ zebrafish were lighter in weight ($P < 0.0001$) (Fig. 1E) and shorter in length ($P < 0.0001$) (Fig. 1F) when compared with *tardbp*$^{+/+}$ siblings. To analyze protein expression, we dissected tissues from three 6-month old *tardbp*$^{fh301/fh301}$ and three *tardbp*$^{+/+}$ siblings and obtained whole cell lysates of brain, eyes, muscle, heart, gills and liver for immunoblotting using the antibody h.TDP-43 Ab2 (which recognizes the C-terminus that is conserved between the human TDP-43 and zebrafish Tardbp). In WT animals, the full-length functional form of Tardbp was detected in all tissues tested including the brain and the eyes (Fig. 1G). In contrast, Tardbp protein was undetectable in tissue extracts from homozygous *tardbp*$^{fh301/fh301}$ animals, indicating that it is full-length *tardbp* null mutant. To exclude the presence of a stable truncated form of the Tardbp protein, we also immunoblotted these samples with an N-terminus Tardbp antibody (h.TDP-43 Ab1) that is raised against the N-terminal 260 amino acids of TDP-43. No bands in the predicted 24 kDa region were observed in the *tardbp* mutants (Fig. 2A), suggesting that the mutant protein is unstable and likely to be rapidly degraded. Thus, the *tardbp*$^{fh301/fh301}$ zebrafish represents a null mutant.

A full-length isoform of *tardbpl* (*tardbpl-FL*) is up-regulated in *tardbp* mutant zebrafish

It has been reported that loss of TDP-43 causes early embryonic lethality in mouse and significant motor deficits in *Drosophila* (20,21). It was therefore surprising that our homozygous mutant *tardbp* animals survived until adulthood with apparently preserved motor function. When we examined the immunoblot of *tardbp*$^{fh301/fh301}$ adult zebrafish with the antibody h.TDP-43 Ab1, we surprisingly observed a 20-fold increase in the ∼43 kDa signal (Fig. 2A, #, and B, $, C, D) in the *tardbp*$^{fh301/fh301}$ fish, instead of the anticipated absence of the ∼43 kDa band corresponding to the full-length Tardbp protein. Since the loss of Tardbp expression has been observed using the h.TDP-43 Ab2 and since zebrafish has only two TDP-43 homologs, we hypothesized that the enhanced ∼43 kDa signal in *tardbp*$^{fh301/fh301}$ lysates might represent a novel isoform transcribed from the *tardbpl* locus. Analysis of the *tardbpl* locus using the GeneScan software (GeneScan, MIT) predicted a novel transcript that produces

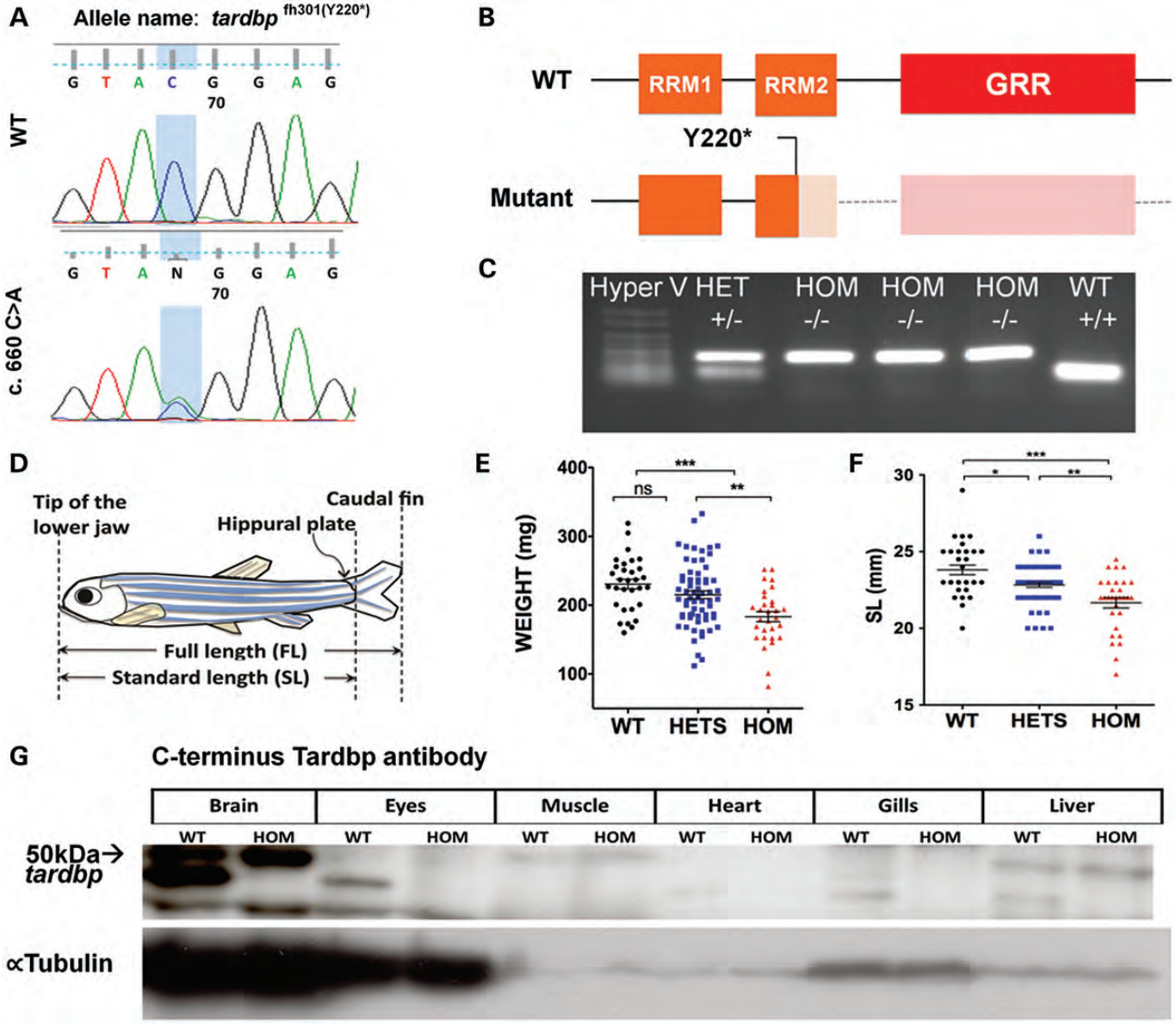

Figure 1. The *tardbp* fh301 mutant (*tardbp*$^{fh301/+}$) zebrafish generated by a TILLING process is viable. (**A**) Through mutation screening of a zebrafish ENU mutagenesis library, a c.660 C>A missense in-frame mutation in *tardbp* was detected. (**B**) The c.660 C>A mutation results in a premature truncation mutation at the 220 amino acids residue (Threonine) in the RRM2 domain. (**C**) c.660 C>A also results in a loss of CViQ1 restriction digest enzyme site, which helps to identify the genotype of the zebrafish following fin clipping. (**D**) Diagrammatic representation of the measurement of SL of zebrafish at 6 months of age. (**E**) Fry from a *tardbp*$^{fh301/+}$heterozygous in cross at F5 generation were fin clipped at 6 months of age to identify the genotype. The weights were significantly different between *tardbp*$^{+/+}$ and *tardbp*$^{fh301/fh301}$ (230 mg, SD $\pm$ 39 versus 183 mg, SD $\pm$ 40, $P < 0.0001$) and *tardbp*$^{fh301/+}$ (215 mg, SD $\pm$ 46, $P < 0.001$). There was no significant weight difference between *tardbp*$^{fh301/+}$and *tardbp*$^{+/+}$ ($P > 0.05$). (**F**) Measurement of the SL revealed significant differences between *tardbp*$^{+/+}$ (23.81 mm, SD $\pm$ 1.76), *tardbp*$^{fh301/+}$ (22.83 mm, SD $\pm$ 1.26) and *tardbp*$^{fh301/fh301}$ (21.67 mm, SD $\pm$ 1.84)(*$P < 0.01$, **$P < 0.001$, ***$P < 0.0001$). (**G**) An immunoblot probed with h.TDP-43 Ab2 (which binds to the C-terminus of TDP-43) demonstrates a loss of Tardbp from all tissues in a 6-month-old adult homozygous mutant zebrafish (*tardbp*$^{fh301/fh301}$). h.TDP-43 Ab2 is specific to Tardbp and does not detect Tardbpl.

an almost full-length Tardbp-like (398 amino acids) protein, which we have named as Tardbpl-FL. The novel *tardbpl-FL* transcript and *tardbpl* share the same translation initiation site.

Earlier, Kabashi *et al.* had shown using the AMO method that knockdown of Tardbpl does not lead to an aberrant phenotype and interpreted this to indicate that the *tardbpl* gene is non-functional (18). Our own studies with AMO targeted to the translation initiation site of *tardbpl* (*tardbpl AMO*) showed that injection of even high doses of *tardbpl AMO* into WT embryos produced no phenotype and the embryos were macroscopically normal at 32 (Fig. 3A–D), 36 and 120 hpf (Supplementary Material, Fig.S2A and C, upper panel). Quantitation of defects in motor axon development also showed that motor axons in *tardbpl* AMO injected WT embryos were normal and indistinguishable from control AMO (CoMo) injected embryos (Supplementary Material, Fig. S2B).

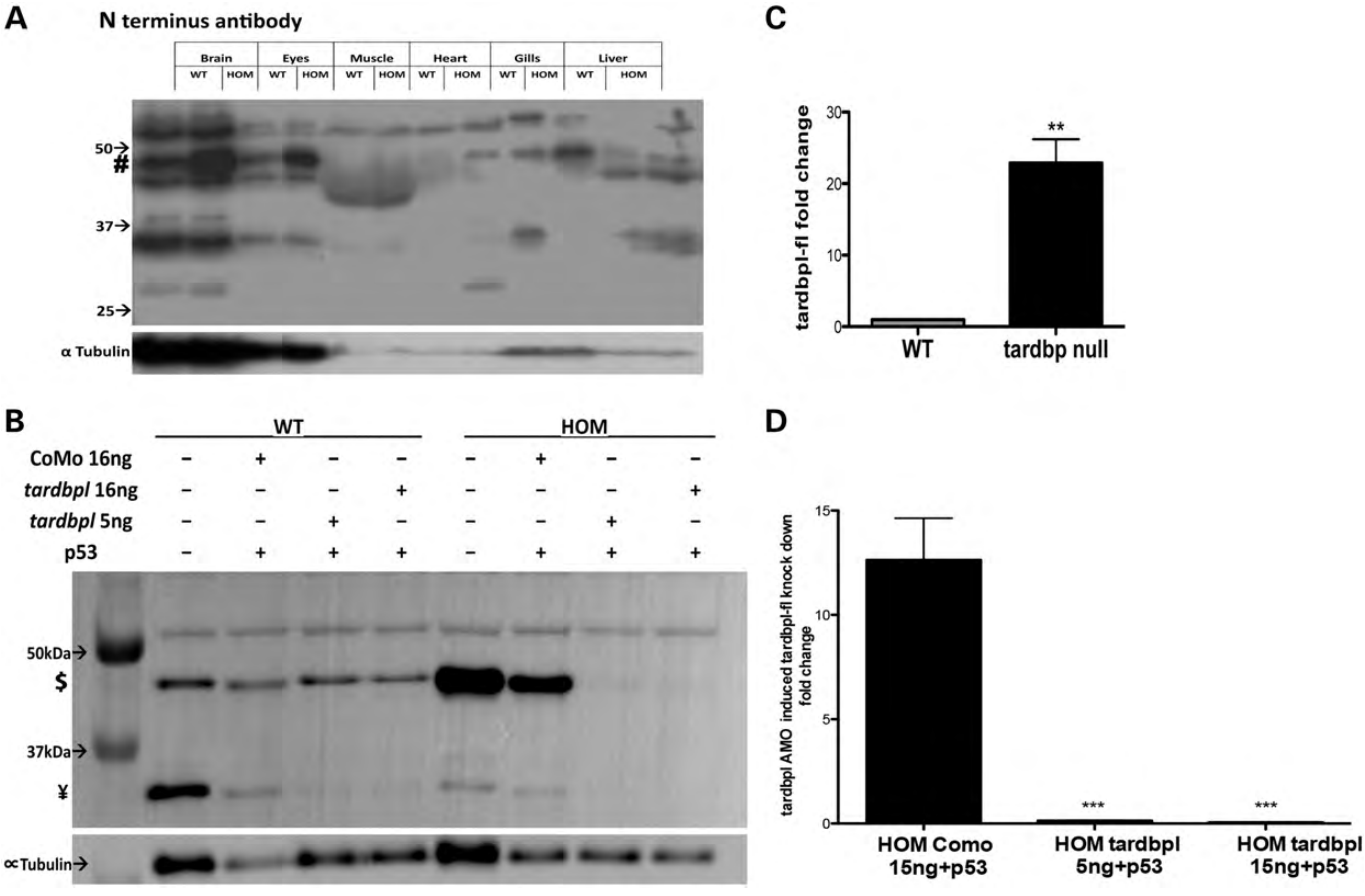

Figure 2. The *tardbp*$^{fh301/fh301}$ null phenotype is rescued by over-expression of a *tardbpl* full-length protein (Tardbpl-FL). (**A**) Western blot of tissues from 6-month-old adult *tardbp*$^{fh301/fh301}$ zebrafish using h.TDP-43 Ab1 which binds to the N-terminus of TDP-43. Compared with the *tardbp*$^{+/+}$, *tardbp*$^{fh301/fh301}$ embryos have an over expressed signal at ∼43 kDa molecular weight indicated by $. This relative over-expression of a protein similar to the molecular weight of Tardbp is present in all the tested tissues of *tardbp*$^{fh301/fh301}$ adult zebrafish. (**B**) *tardbpl* AMO injection into *tardbp*$^{fh301/fh301}$ fish resulted in near complete (5 ng) and complete (16 ng) knockdown of Tardbpl-FL over expression, and Tardbpl (∼33 kDa, indicated by ¥) suggesting that *tardbpl* and *tardbpl-FL* share a similar translational initiating region. (**C**) Tardbpl-FL protein is upregulated 20-fold in the *tardbp*$^{fh301/fh301}$compared with the *tardbp*$^{+/+}$($P < 0.001$). (**D**) Tardbpl-FL and Tardbpl are knocked down by *tardbpl* AMO injection in *tardbp*$^{fh301/fh301}$ embryos ($P < 0.0001$).

To investigate whether this novel *tardbpl-FL* transcript from the *tardbpl* locus is rescuing the *tardbp* mutant (*tardbp*$^{fh301/fh301}$), we knocked down the expression of the novel isoform in *tardbp*$^{fh301/fh301}$(homozygous) embryos by injecting a *tardbpl AMO*. Protein homogenates extracted from the *tardbp*$^{fh301/fh301}$ and WT embryos (*tardbp*$^{+/+}$ sibling in-cross) microinjected with *tardbpl AMO* at 36 hpf were probed with h.TDP-43 Ab1. Near complete (with 5 ng of *tardbpl AMO*) and complete (with 16 ng of *tardbpl AMO*) knockdown of the ∼43 kDa signal (Tardbp-FL novel protein) was observed in the *tardbp*$^{fh301/fh301}$ embryos compared with the control AMO (CoMo) injected and the uninjected groups ($P < 0.0001$) (Fig. 2B $, 2C and D). However, no change in the 43 kDa band (representing the Tardbp protein) was observed in *tardbpl AMO* injected WT embryos (Fig. 2B). These findings indicate that the ∼43 kDa protein form is specifically upregulated in the *tardbp*$^{fh301/fh301}$mutant embryos and is encoded by the *tardbpl-FL* transcript. The reduction of the 33 kDa Tardbpl band in both *tardbp*$^{fh301/fh301}$ and WT embryos, following *tardbpl AMO* injection (Fig. 2B, ¥), indicates that the zebrafish *tardbpl* locus can encode protein isoforms of two differing lengths, the short (33 kDa) Tardbpl and the full-length (43 KDa) Tardbpl-FL protein.

tardbp and *tardbpl-FL* double knockouts have reduced survival and develop motor defects

Earlier, we saw that knockdown of Tardbpl in WT embryos produced no phenotype, indicating that the truncated 33 kDa Tardbpl protein is probably non-functional. However, complete knockdown of Tardbpl-FL using 16 ng of *tardbpl AMO* (Fig. 2B $, 2C and D) in *tardbp*$^{fh301/fh301}$ embryos resulted in morphological abnormalities (a curly tail phenotype) as early as 32 hpf ($P < 0.0001$) (Fig. 3H and I), whereas 5 ng of *tardbpl AMO* produced a less severe phenotype ($P < 0.0001$) (Fig. 3G and I). This phenotype progressively worsened over time (Supplementary Material, Fig. S2C). Complete knockdown of Tardbpl-FL in the *tardbp*$^{fh301/fh301}$ embryos resulted in significantly reduced survival (all double morphant/mutant embryos died by 10 dpf) ($P < 0.0001$) compared with those injected with control AMO (CoMo) (Fig. 3J).

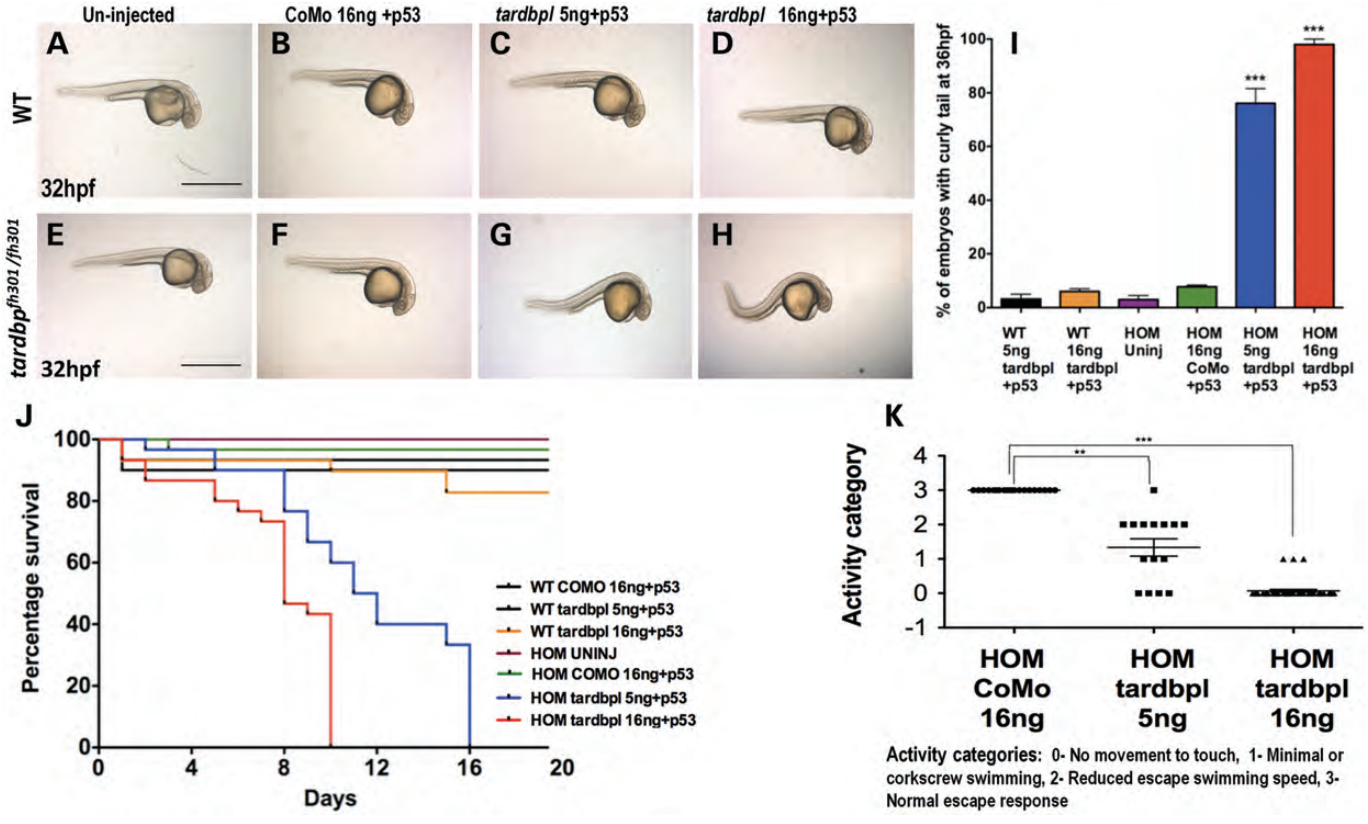

Figure 3. Effects of Tardbpl-FL knockdown in WT and *tardbp* null zebrafish embryos. (**A**–**D**) Uninjected, control AMO (CoMo) injected and *tardbpl AMO* with *p53 (tardbpl* AMO +*p53)* groups of WT (*tardbp*$^{+/+}$) embryos were morphologically normal when compared with *tardbpl AMO* with *p53* injected HOM (*tardbp*$^{fh301/fh301}$ embryos) zebrafish (**E**–**H**) which develop a curly tail phenotype at 32 hpf ($P < 0.0001$) (**I**). (**J**) Knockout of Tardbp and Tardbpl/Tardbpl-FL significantly reduces survival of *tardbp*$^{fh301/fh301}$ embryos to 10 dpf (16 ng) and 16 dpf (5 ng) and both Kaplan–Meier curves are statistically significant compared with the control AMO (COMO)+p53 injected group ($P < 0.001$). (**K**) The double knockout zebrafish also had a significantly reduced escape response ($P < 0.0001$), demonstrating a motor behavioral defect caused by loss of both Tardbp and Tardbpl-FL.

The animals injected with the lower dose (5 ng *tardbpl AMO*) survived slightly longer but had to be sacrificed when they showed an inability to swim or feed (Fig. 3J). The double mutants also had a significantly reduced escape response ($P < 0.0001$), demonstrating a motor behavioral defect caused by loss of both Tardbp and Tardbpl-FL (Fig. 3K).

Simultaneous loss of Tardbp and Tardbpl-FL results in significant axonal path finding defects

It is well established that mutations in the human *TARDBP* gene are associated with ALS and are, therefore, deleterious to motor neurons. However, there was no significant difference in the motor axonal morphology between *tardbp*$^{fh301/fh301}$ and WT control fish at 36 hpf (Fig. 4A–C) and the control *AMO* (CoMo) injected groups (Fig. 4D–F). Additionally, motor axon development was completely normal in WT embryos injected with *tardbpl AMO* (Fig. 4 G, J and M and Supplementary Material, Fig. S2B). We therefore analyzed the effects of loss of both Tardbp and Tardbpl-FL on motor axons of the *tardbp* mutant. Knockdown of Tardbpl-FL with 16 ng *tardbpl AMO* in *tardbp*$^{fh301/fh301}$ embryos resulted in a complete arrest of axonal outgrowth at 36 hpf ($P < 0.0001$) (Fig. 4K, L and N). A less severe axonal path finding defect was observed with a lower dose (5 ng, $P < 0.001$) of *tardbpl AMO* (Fig. 4H and I). Taken together, these findings confirm that *tardbpl-FL* is able to compensate for the loss of *tardbp*. Expression of Tardbpl-FL in *tardbp*$^{fh301/fh301}$ mutants showed that this novel transcript is expressed right from the earliest stages of development, indicating that it may be stored maternally in the oocyte, with continued endogenous expression during development (Supplementary Material, Fig. S3).

tardbpl-FL is a novel alternatively spliced *tardbpl* transcript

The basal level of Tardbpl (33 kDa isoform) is higher in WT zebrafish compared with *tardbp*$^{fh301/fh301}$ zebrafish (Fig. 2C, ¥ and 5A,*). The reduced level of Tardbpl in the mutant may correlate with the compensatory upregulation of Tardbpl-FL (43 kDa isoform). We postulated that alternative splicing of *tardbpl* could generate the two forms (Fig. 5B and C). Following alignment of exon–intron boundaries of the GeneScan predicted *tardbpl* transcript with the exons and introns of *tardbpl*, we determined that the novel transcript could be generated by alternative splicing. Both splice isoforms share nucleotide identity at the translation initiation site, consistent with the finding that the *tardbpl AMO* knocks down both

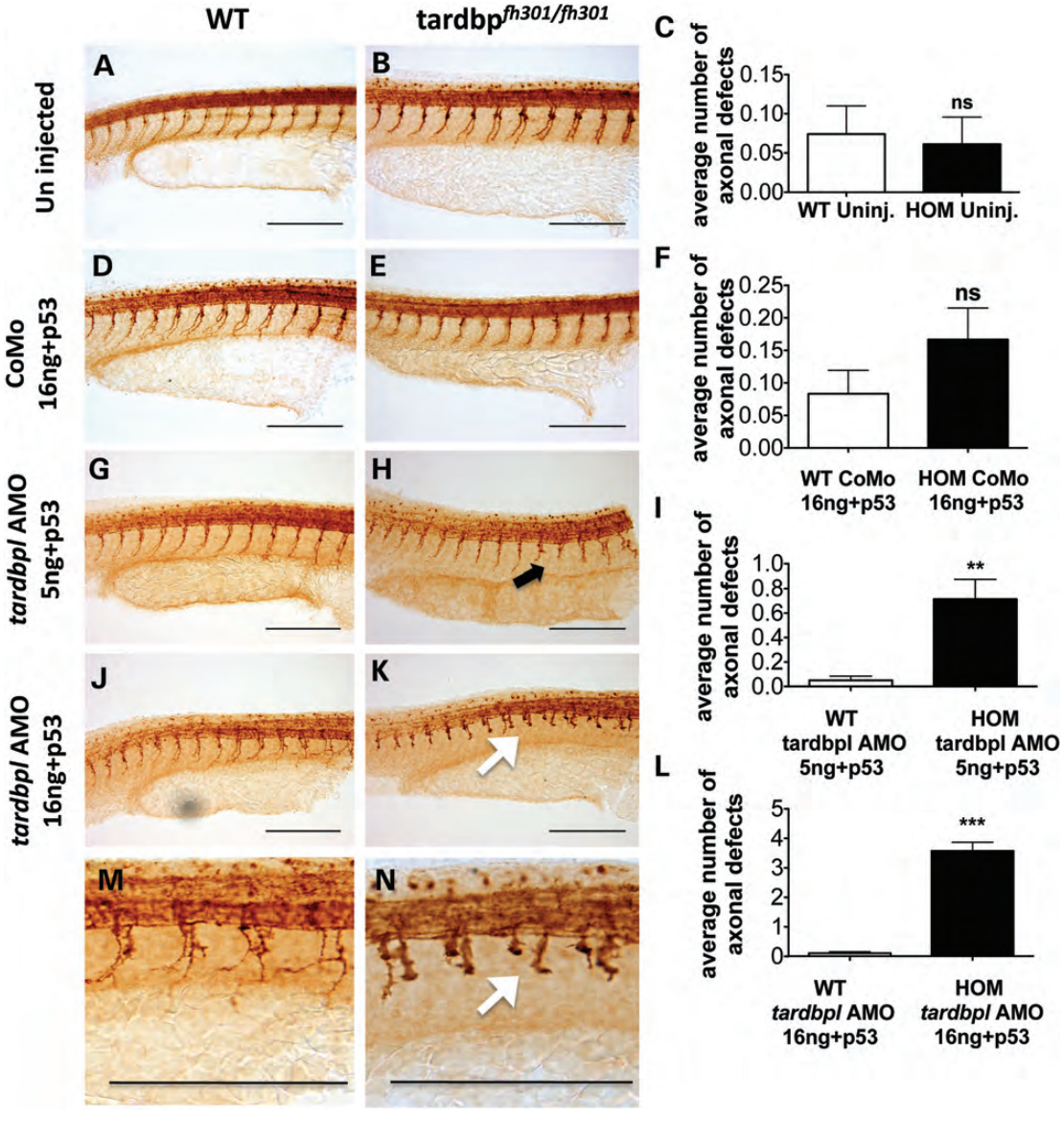

Figure 4. Motor axons are abnormal in Tardbpl-FL knocked down *tardbp*$^{fh301/fh301}$ embryos at 36 hpf. Lateral views of the whole-mounted *tardbp*$^{+/+}$ and *tardbp*$^{fh301/fh301}$ embryos stained with znp-1 to detect axons. (**A**–**C**) Uninjected *tardbp*$^{+/+}$ (WT) and *tardbp*$^{fh301/fh301}$ do not show any significant difference in axonal defects similar to *control AMO (CoMo)* injected groups (**D**–**F**). (**G**–**I**) Partial knockdown of Tardbpl-FL with *tardbpl* AMO +*p53* results in a significant rise in the axonal defects in the *tardbp*$^{fh301/fh301}$ mutant zebrafish ($P < 0.001$). (J) Normal motor axons in *tardbp*$^{+/+}$ injected with *tardbpl AMO 16* ng. (**K**) Complete knockdown of *tardbpl-FL* in *the tardbp*$^{fh301/fh301}$ resulted in severe axonal outgrowth defects with complete arrest of axons at the horizontal myoseptum ($P < 0.0001$) (**L**). (**M** and **N**) Enlarged sections of (**J** and **K**) demonstrating severe axonal out growth defects in the double knockout (Tardbp and Tardbl-FL) embryos. Black arrow points out at an infrequent axonal truncation defect (low dose *tardbpl* AMO), while white arrows indicate numerous axonal out growth defects (high dose *tardbpl* AMO).

Tardbpl and Tardbpl-FL (Fig. 2B, $ and ¥). We performed qRT–PCR, using transcript-specific primers designed across exon–exon boundaries, to quantify the relative abundance of the two splice isoforms, *tardbpl* and *tardbpl-FL*. An internal primer set was designed to cross the exon 2–3 boundaries in the 5′ end of the gene, which is common to both *tardbpl and tardbpl-FL*. Complementary DNA (cDNA) amplified using the RNA extracted from both *tardbp*$^{+/+}$ (WT) and *tardbp*$^{fh301/fh301}$ (HOM) embryos showed that in the *tardbp*$^{fh301/fh301}$ embryos, *tardbpl-FL* is over-expressed by as much as 2.4-fold (ΔΔ CT, WT-HOM *tardbp*$^{fh301/fh301}$ +1.27), while *tardbpl* expression is reduced by 0.8-fold (ΔΔ CT, WT-HOM *tardbp*$^{fh301/fh301}$ −0.21)(Fig. 5D) (Supplementary Material, Fig. S4). These data confirm that *tardbpl* is indeed alternatively spliced to generate the newly identified *tardbpl-FL* transcript.

DISCUSSION

TDP-43 is one of the key proteins involved in the pathogenesis of FTLD-U and ALS (22). The importance of TDP-43-related

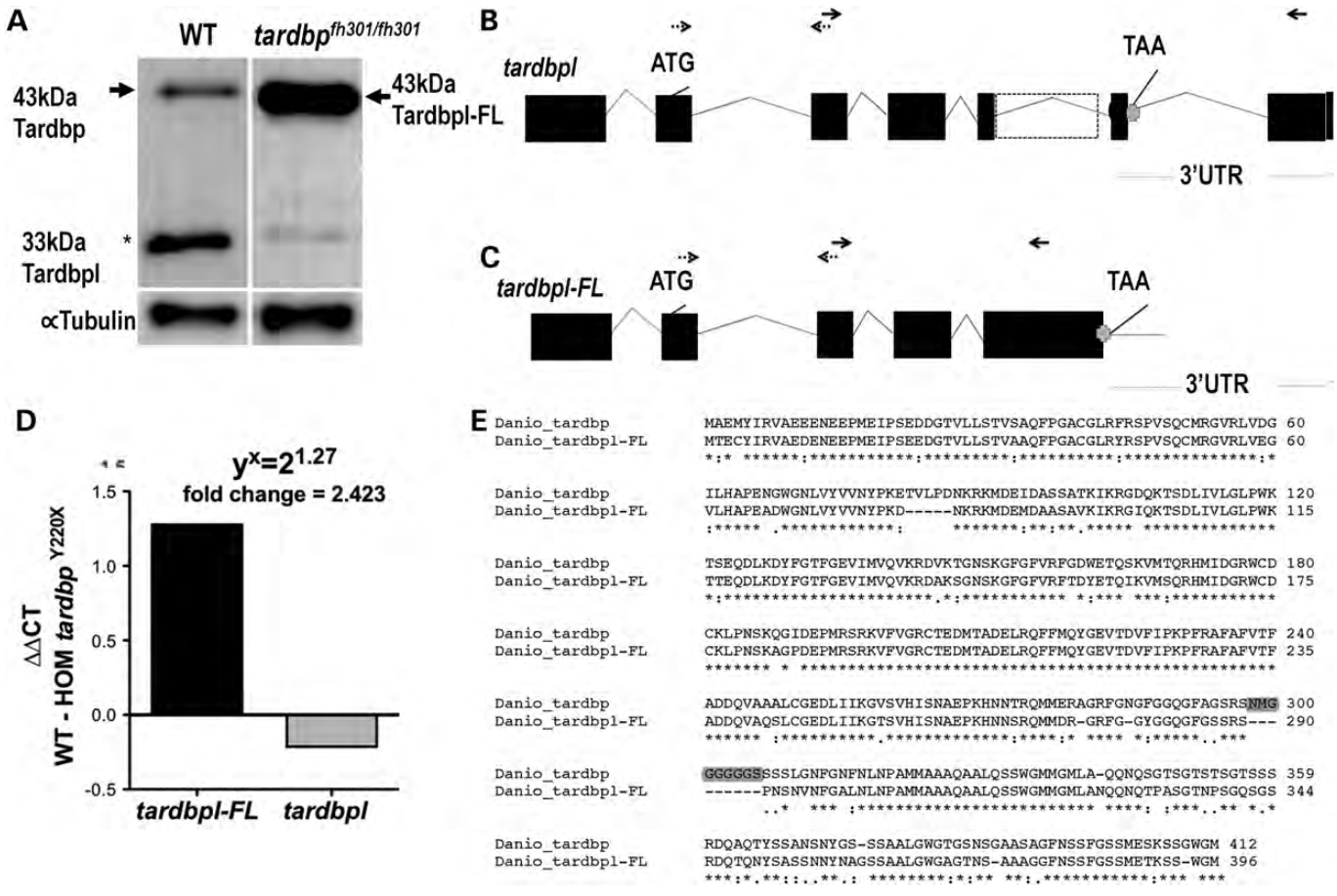

Figure 5. Alternative splicing of *tardbpl* gives rise to *tardbpl-FL*, which rescues the *tardbp*$^{fh301/fh301}$ null phenotype. (**A**)Western blot of WT and *tardbp*$^{fh301/fh301}$ embryos at 48 hpf, probed with h.TDP-43 Ab1, demonstrating relative over expression of Tardbpl-FL (solid black arrow) and the reduction in Tardbpl expression in the *tardbp*$^{fh301/fh301}$ mutant zebrafish (asterisk). (**B**) Introns 5–6 of the *tardbpl* (ENSDART00000027255) on chromosome 23 contain a coding sequence, which potentially could give rise to a longer Tardbpl protein (Tardbpl-FL). (**C**) Predicted alternative splicing event, which results in inclusion of introns 5–6 creating *tardbpl-FL*. RT–PCR primers for common exon (exons 2 and 3), tardbpl-FL-specific primers (exons 4 and 5 but within intron 6 of tardbpl) and tardbpl-specific primer (exons 4 and 7) are also shown by arrows. (**D**) qRT–PCR estimation of expression of *tardbpl* and *tardbpl-FL* revealed a 2.42-fold increase (*tardbpl-FL*, ΔΔCT WT-*tardbp*$^{fh301/fh301}$ of +1.27) in the *tardbpl-FL* expression in *tardbp*$^{fh301/fh301}$mutant embryos compared with the WT embryos at 48 hpf and *tardbpl* expression was reduced in the *tardbp*$^{fh301/fh301}$mutant embryos (*tardbpl*, ΔΔCT WT-*tardbp*$^{fh301/fh301}$ of −0.213). (**E**) ClustalW2 alignment of the Tardbp and predicted Tardbpl-FL amino acid sequences. Both the N and the C termini are highly conserved. Tardbpl-FL is missing nine amino acids from the GRD, of which six are glycine residues (highlighted in grey).

pathology in ALS and FTLD-U has been reinforced by the recent discovery, showing that TDP-43 pathology predominates in ALS and FTLD cases with an intronic hexanucleotide repeat expansion in *C9ORF72*, which accounts for up to 50% of fALS and 7–10% of sALS cases (23–25). Aggregate formation with C-terminus truncated, hyperphosphorylated TDP-43 and a dramatic redistribution of nuclear TDP-43 to the cytoplasm of surviving motor neurons in pathological samples have been consistently observed (3). This reduction of normal nuclear expression of TDP-43 may affect vital nuclear functions such as transcription and post-transcriptional regulation of gene expression, including alternative splicing (26). Therefore a strong case exists to investigate the loss of function as a potential mechanism of TDP-43-related pathology.

Here, we describe the first stable mutant *TDP-43* (*tardbp*) zebrafish model of ALS by TILLING. The loss of TDP-43 has been shown to cause embryonic lethality in mice (20) and fruit-fly (10). Additionally, Kabashi *et al.* showed that morpholino-mediated transient knockdown of Tardbp was shown to produce a severe impairment of motor axon growth and development (18). Thus, it was surprising to observe normal Mendelian ratios maintained among homozygous (*tardbp*$^{fh301/fh301}$), heterozygous (*tardbp*$^{fh301/+}$) and WT (*tardbp*$^{+/+}$) zebrafish generated from a heterozygous (*tardbp*$^{fh301/+}$) in cross, and survival of homozygous mutant (*tardbp*$^{fh301/fh301}$) animals to adulthood. To ensure that earlier morpholino studies reproduced in our hands, we used identical morpholinos to that used in the Kabashi study, and we also observed that AMO knockdown of Tardbp using the translation blocking AMO produced severely defective embryos when injected in both WT and the *tardbp*^{fh301} mutants (Supplementary Material, Fig. S5E and F). However, even when we used the highest dose of a splice blocking AMO, which completely eliminated the WT splice form of Tardbp (Supplementary Material, Fig. S5B), we saw that the embryos were apparently normal (Supplementary

Material, Fig. S5G and H). Thus, we believe that the translation blocking AMO experiments may have some off-target mediated effects that could have contributed to the observed phenotype. Although morpholino (AMO)-based approaches have in general been useful for the characterization of gene function, here we present a scenario where generation of a stable mutant but not the AMO approach was useful in identifying the function of a duplicated gene. This highlights one potential pitfall of using purely morpholino-based approaches to study gene function and indicates that a combined approach may add value in some circumstances.

The upregulation of a novel isoform from the *tardbpl* locus shown in our studies supports the idea that compensation by the *tardbpl* locus in the *tardbp* mutants may explain the viability of these mutants. Here, we show that the loss of full-length Tardbp in the *tardbp*$^{fh301/fh301}$animals leads to enhanced alternative splicing of *tardbpl* to generate a novel transcript *tardbpl-FL*, indicating the existence of a newly identified regulatory loop that controls Tardbp levels in zebrafish. In addition, we demonstrate that knockdown of both Tardbp and Tardbpl-FL leads to severe defects in motor neuronal development, therefore establishing a vital role for Tardbp in motor neuron and axon development. Studies *in vitro* have shown that TDP-43 knockdown in a neuronal cell line using small interfering RNA (siRNA) resulted in neurite out growth defects and increased cell death (27). Abnormal axonogenesis has also been observed in a variety of zebrafish models of motor neuron disease and in sod1 mouse models of ALS (28–30). Axonal changes are reflected much earlier than motor neuron loss in ALS and the abnormal axonal development may reflect some underlying sensitivity of motor axons to these mutations. This provides a novel, tractable vertebrate model for the analysis of the physiological consequences of the loss of Tardbp in a small vertebrate model that is amenable for studying disease processes *in vivo* at single neuron resolution and for high throughput drug and genetic screens.

It is noteworthy that humans also have two *TARDBP* genes; one is located on chromosome 1p36.22 (*TARDBP*) while the other is a pseudogene located on chromosome 20p12.3 (*TARDBPP1*). The *tardbp* gene in zebrafish is located on chromosome 6 and the *tardbpl* gene is located on chromosome 23. Zebrafish and humans appear to share ancestral chromosomes (31). We compared the synteny map of the *tardbp* and *tardbpl* loci in zebrafish with those of the human and mouse genes and the pseudogenes, and found partial conservation of synteny in both cases. However, genes around the zebrafish *tardbp* locus were less rearranged compared to those at the *tardbpl* locus (Supplementary Material, Fig. S6). The zebrafish chromosome 23 is extensively recombined and relevant genes are distributed amongst many other chromosomes in humans (such as 1,2,6,12,20 and X), with a component on chromosome 20, where the human *TARDBPP1* gene is located. Similarly in the mouse, near the syntenic region of human chromosome 20 (mouse chromosome 2), we are able to locate a *Tardbp* pseudogene (GM13886). Thus, it is likely that '*tardbpl'* in humans and mice underwent recombination events that could have potentially led to the loss of functional *tardbpl* and the creation of the *TARDBPP1* pseudogene and GM13886 respectively.

It is of interest to question what selection pressure enabled the maintenance of functional *tardbp* and *tardbp-FL* genes in zebrafish. One interesting clue suggesting divergent roles for Tardbp and Tardbpl-FL is the phenotype of the *tardbp*$^{fh301/fh301}$ mutants. We observed that despite the upregulation of *tardbpl-FL* in the *tardbp*$^{fh301/fh301}$ mutant zebrafish, the mutants were smaller in size compared with WT (Fig. 1), which indicates that *tardbp* and *tardbpl* may have both functionally overlapping and distinct roles in zebrafish development and in adult life. The small body phenotype of *tardbp*$^{fh301/fh301}$ animals suggests that *tardbp* may play a critical role in growth regulation, which is not fully compensated by the upregulation of *tardbpl-FL* expression in the mutants. In keeping with this are the findings from conditional postnatal knockout of *Tardbp* in mice which showed that these mice develop loss of body weight and down regulation of Tbc1d1, increased expression of which is associated with obesity (32). Thus, the specialized role played by *tardbp* when compared with *tardbpl* may have been important in maintaining the two genes during evolution. As we do not yet have a stable *tardbpl* mutant, we do not yet know what specific role *tardbpl-FL* may play in zebrafish development.

Upregulation of Tardbpl-FL expression by alternative splicing of the *tardbpl* locus in the *tardbp*$^{fh301/fh301}$ mutants is interesting. It was recently shown that autoregulation of *TARDBP* involved a 3′UTR TARDBP binding site that under high TARDBP conditions led to increased intron 6 splicing and RNA polymerase stalling resulting in a shorter *TARDBP* ORF, V2 *TARDBP* transcript that is degraded by a nonsense-mediated decay. Under conditions of low TARDBP expression, this mechanism occurs at a low efficiency, thus promoting the stable longer V1pA4 and V1pA1 *TARDBP* transcript which makes the full-length protein (33,34). The generation of the *tardbpl-FL* transcript occurs by the inclusion of intron 5 of *tardbpl*, which is able to code for the additional C-terminal amino acids generating an almost full-length Tardbp-like protein and exclusion of exons 6 and 7. Intron 5 contains a UGUGU motif near the splice donor site of exon 6. Additionally, another canonical high affinity TDP-43 binding site $-(GU)_6$ is located in intron 6 which is the 3′UTR region of the *tardbpl-FL* transcript. Although the UGUGU motif is not a canonical high affinity RNA binding site of TDP-43, it has the elements required for interacting with TDP-43 during splicing (35). A loss of Tardbp (condition of low Tardbp expression) could potentially regulate the *tardbpl/tardbpl-FL* splicing process, by allowing intron 5 inclusion, and eliminating intron 6 splicing, thus producing the *tardbpl-FL* transcript. Taken together, these results predict an *in vivo* auto-regulatory model involving *tardbp* and *tardbpl/tardbpl-FL* in keeping with the type of auto-regulatory mechanism/s hypothesized for TDP-43(33,34). Although this alternative splicing of *tardbpl* is zebrafish specific, it provides a good model system to study differential splicing by *tardbp*.

One interesting aspect of the upregulation of Tardbpl-FL expression is that it is unable to completely rescue the loss of Tardbp. Tardbpl-FL lacks nine residues from the glycine-rich domain (GRD) of which six are glycine residues. Two interesting observations in this model over-expressing tardbpl-FL are evident. First, despite the high homology between Tardbpl-FL and Tardbp, Tardbpl-FL is unable

to auto-regulate itself, resulting in a massive 20-fold upregulation of the Tardbpl-FL protein. Second, an observation from TDP-43 over expression *in vitro* and *in vivo* models is that over-expression of full-length WT, mutant TDP-43 or C terminal fragments of TDP-43 are all toxic and/or lethal (17,36). The toxicity of over-expression of exogenous TDP-43 even at relatively low levels in transgenic rodents (37,38) is not observed in the *tardbp*$^{fh301/fh301}$ null zebrafish with compensatory 20-fold increase in the Tardbpl-FL protein level. Therefore, it is plausible that the glycine residues which are missing from the GRD of the Tardbpl-FL (Fig. 5E shaded in grey) are indeed important for efficient tardbp slicing and potentially for mediating the toxicity of tardbp.

Taken together, our data describe for the first time, a critical role for *tardbp* and *tardbpl* in zebrafish development. We show that *tardbp* is important in the regulation of body size as over-expression of Tardbpl-FL in the *tardbp*$^{fh301/fh301}$ mutants is unable to rectify this deficit. However, increased *tardbp-FL* expression in *tardbp*$^{fh301/fh301}$ mutants is able to partially compensate for the early developmental role of *tardbp*. The complete knockdown of *tardbp* and *tardbpl-FL* results in severely abnormal motor neuronal development and concurrent embryonic lethality, demonstrating a critical role for Tardbp or Tardbpl-FL in embryonic neurodevelopment. The uncovering of a newly identified regulatory loop between *tardbp* and *tardbpl* and the discovery of *tardbpl-FL* in zebrafish will allow us to use the double knockdown zebrafish model to study disease mechanisms and neuroprotective strategies and to better understand human ALS associated with *TARDBP* mutations.

MATERIALS AND METHODS

Zebrafish husbandry

Adult zebrafish and embryos were raised at 28.5°C. WT animals were from the AB strain. Embryo collections, AMO (antisense morpholino oligonucleotide) microinjection and maintenance of the mutant and WT zebrafish lines were carried out according to the standard protocols and in accordance with UK Animals (Scientific Procedures) Act 1986. The *tardbp*Y220X, mutant (*tardbp*^{fh301}) line was generated using the TILLING process undertaken in the Fred Hutchinson Cancer Research Center, Seattle, USA, under Animal Care protocol 1342, which is reviewed and approved annually by the FHCRC Institutional Animal Care and Use Committee and is in accordance with the recommendations of the American Veterinary Association.

Generation of a *tardbp* nonsense allele (*tardbp*^{fh301})

The ***tardbp***^{fh301} mutant was generated in the AB background and identified in a TILLING screen. The mutant was recovered by *in vitro* fertilization of AB eggs using a cryo-preserved sperm sample from a single heterozygous F1 male. Heterozygous F1 adults were out-crossed into the AB background and heterozygous F2 adult fish identified by fin clipping and genotyping. The F2 heterozygous (*tardbp*$^{fh301/+}$) animals were bred with AB fish for three further generations to obtain F5 mutant heterozygotes. All experiments were carried out on F6 progeny homozygous for the c.660 C>A (*tardbp*$^{fh301/fh301}$) and their WT (*tardbp*$^{+/+}$) siblings.

Fin clipping, genotyping by PCR and measurement of weight and length of adult zebrafish

Adult zebrafish at 3 months were fin clipped to identify the genotype as previously described (39). At the same time, anesthetized fish were weighed and measured from the tip of the lower jaw to the end of the hipural plate. Once the genotyping results were available, fish were grouped into tanks of their respective genotype. DNA was extracted using a DNAeasy kit (Qiagen). A pair of primers was designed (*tardbp*_genFWD 5′CAAGGTATAGATGAACCAATGAGG A_3′ and *tardbp*_genREV 5 GTCATCTGCAAAGGTG ACAAAAG 3′) for PCR amplification of the extracted DNA. The PCR mixture was digested overnight with CVQI at 25°C. The genotypes were identified based on fragment sizes after gel electrophoresis. In initial experiments, DNA extracted and genotyped using CViQI, as above, was also sequenced to verify the mutation.

Assessment of the swimming of the larvae

Swimming behavior of the larvae at 5 dpf was assessed. Larvae were probed externally and their escape response was analyzed. The escape response was classified into four categories: normal swimming (3), reduced speed (2), corkscrew movement or minimal movement (1) and no movement (0).

Biochemistry and immunoblotting

Six-month-old homozygous (HOM) (*tardbp*$^{fh301/fh301}$) and WT adult zebrafish (four zebrafish per group) were sacrificed using 2% Tricaine (Sigma, UK) to obtain brain, spinal cord, eyes, muscle, heart, gills and liver for protein and RNA extraction. Protein extraction from embryos was carried out at 36 hpf or 48 hpf. At least 100 embryos were collected for each category studied and deeply anesthetized as for adult zebrafish with Tricaine. Protein extraction from samples was carried out as previously described with minor modifications (16). The membranes were probed with an anti-human TDP-43 antibody 1 (N-terminal 1–260 amino acids) and TDP-43 antibody 2 (last 160 amino acids of the C terminus) (both from Proteintech) which we will refer to as h.TDP-43 Ab1 (1:1200) and h.TDP-43 Ab2 (1:1500), respectively, in the article. The h.TDP-43 Ab1 is predicted to detect both the Tardbp and Tardbpl proteins because of the homology of the N-terminal regions of these proteins, whereas the C-terminal antibody h.TDP-43 Ab2 will detect Tardbp but not Tardbpl. Alpha-tubulin expression was used as the loading control (1:10,000) (Sigma). Immunoblots were developed using the ECL detection kit (GELifesciences.com) and the G box hardware and software which were also used for densitometry (Integrated Scientific Solutions, San Diego, CA, USA).

Antisense morpholino oligonucleotide (AMO) mediated knockdown of *tardbpl*

A translation-blocking AMO was designed to knockdown *tardbpl* (*tardbpl* AMO) (5′-CCACACGAATATAGCACTCC GTCAT-3′). The standard control AMO (CoMo) (Genetools, LLC, Philomath, OR, US A*)* was also used to distinguish the specificity of the effects seen from the knockdown of *tardbpl*. Furthermore an AMO against zebrafish tumor suppressor p53 (p53) gene (*p53 AMO*) was also used along with the *tardbpl* AMO (Genetools). The AMO was dissolved in nuclease-free sterile water to obtain a stock solution of 4 nmol/μl. The optimal dose was established by injecting a range of *tardbpl* AMO concentrations along with 8 ng of p53 AMO. To monitor the accuracy of injections, phenol red (Sigma) was added at a final concentration of 1% prior to injecting the zebrafish embryos. One nanoliter of the optimal AMO dilution was injected into the yolk sac of the embryos at the one to two cell stage. Survival of the embryos injected with *tardbpl* AMO, control AMO (CoMo) and uninjected controls was monitored for 72 hpf. Embryos were observed at 4, 8, 24, 32–36, 48 and 72 hpf for any obvious morphological changes. At least four independent experiments were carried out per injection category and each experimental repeat included at least 100 embryos per category. Embryos were then processed as required for immunohistochemistry and immunoblotting.

Immunohistochemistry on whole-mount embryos

Immunohistochemistry was carried out on whole-mount 36 hpf embryos as previously described (40). The znp-1 mouse monoclonal antibody (1:400) was used to label motor axons, and mouse anti-islet-1 to identify neuronal cell bodies (both from DSHB, University of Iowa, USA). Motor axonal projection defects were assessed by counting the number of axons that were either prematurely truncated or abnormally branched at or just below the horizontal myoseptum. A total of 10 axons in both hemi-segments of each zebrafish were counted immediately caudal to the yolk bulge to standardize the counting across all groups. Each hemi-segment was scored out of 10 for the number of axons with premature truncating or branching or both defects. At least 30 embryos per category for each of four experimental repeats were counted. The number of motor neurons and Rohon Beard neurons stained with islet-1 were counted across eight myo-segments from immediately caudal to the yolk bulge to the end of the yolk extension. Images were obtained using a Zeiss light microscope with bright field settings. Images were analyzed using NIH Image J (Rasband, W.S., ImageJ, US National Institutes of Health, Bethesda, MD, USA, http://imagej.nih.gov/ij/, 1997–20120) software.

RNA extraction and quantitative real time PCR (qRT-PCR)

Tissues from adult zebrafish or embryos were obtained as described earlier and total RNA was extracted using the Trizol reagent (Invitrogen, UK). One microgram of RNA was used for the synthesis of first-strand cDNA synthesis. Gene-specific primers were designed for *tardbpl* (forward 5′-CGTCACCTTCGCAGACGATCAGGTT-3′ and reverse 5′-GCCTAAGCACAATAATATTCATCACCTCTTTTCCAA TT-3′, *tardbpl-FL* (forward 5′-CGTCACCTTCGCAGACG ATCAGGTT-3′ and reverse 5′-GCCCACGATCCATCATTT GCCTACTATT-3′). A set of primers, which amplifies a common sequence within both *tardbpl* and *tardbpl-FL*, were used as an internal control for qRT-PCR (forward 5′–TCT GGTGTACGTGGTTAATTATCCAAAAGATAACA-3′ and the reverse 5′-AGAGGTGATCATGGTGCAGGTGAAAAG). Two housekeeping genes, which have been well characterized for use in zebrafish [EF1alpha, forward (5′-CTGGAGGCC AGCTCAAACAT-3′), reverse (5′-ATCAAGAAGAGTAGT ACCGCTAGCATTAC-3′) and RP113 alpha, forward (5′-T CTGGAGGACTGTAAGAGGTATGC-3′), reverse (5′–AGA CGCACAATCTTGAGAGCAG-3′)] were used for standardizing the qRT–PCR results as previously described (41). Primers were optimized and efficiency assessed by analyzing the standard curves. A real-time PCR was performed using an ABI Prism 7900 HT sequence detection system (Applied Biosystems) using an Evergreen fluorescent label.

Statistical analysis

When three or more groups were compared, one-way ANOVA, with Kruskal–Wallis statistic and with Dunn's multiple comparison testing as appropriate, was used. When only two groups were compared, a paired *t*-test was used. The results of three independent experiments were used in every analysis.

AUTHOR CONTRIBUTION

C.A.A.H. performed the experimental work, analyzed all the data and drafted the manuscript; A.J.G. and P.W.I. were co-supervisors on the project; A.J.G. designed experiments, analysed data and helped draft the manuscript; T.P.M., L.P. and C.B.M. created the tilled mutant; P.J.S. and T.M.R. oversaw the project, analyzed all the data and wrote the manuscript.

SUPPLEMENTARY MATERIAL

Supplementary Material is available at *HMG* online.

Conflict of Interest statement. None declared.

FUNDING

C.A.A.H. is a UK Medical Research Council (MRC) Clinical Research Fellow funded by MRC Centre grant G0700091 awarded to P.W.I. TILLING of *tardbp* was supported by NIH RO1 HG002995 to C.B.M. C.B.M. is an investigator with the Howard Hughes Medical Institute. T.R. and P.J.S. are funded by the Motor Neuron Disease Association (MNDA) UK and Thierry Latran Foundation, France. P.J.S. is supported by a EU Framework 7 Systems Biology award: grant number 259867. Funding to pay the Open Access publication charges for this article was provided by Medical Research Council, UK, Center Grant # G0700091.

REFERENCES

1. Ferraiuolo, L., Kirby, J., Grierson, A.J., Sendtner, M. and Shaw, P.J. (2011) Molecular pathways of motor neuron injury in amyotrophic lateral sclerosis. *Nat. Rev. Neurol.*, **7**, 616–630.
2. Lagier-Tourenne, C., Polymenidou, M. and Cleveland, D.W. (2010) TDP-43 and FUS/TLS, emerging roles in RNA processing and neurodegeneration. *Hum. Mol. Genet.*, **19**, R46–R64.
3. Neumann, M., Sampathu, D.M., Kwong, L.K., Truax, A.C., Micsenyi, M.C., Chou, T.T., Bruce, J., Schuck, T., Grossman, M., Clark, C.M. *et al.* (2006) Ubiquitinated TDP-43 in frontotemporal lobar degeneration and amyotrophic lateral sclerosis. *Science*, **314**, 130–133.
4. Geser, F., Lee, V.M. and Trojanowski, J.Q. (2010) Amyotrophic lateral sclerosis and frontotemporal lobar degeneration, a spectrum of TDP-43 proteinopathies. *Neuropathology*, **30**, 103–112.
5. Wegorzewska, I. and Baloh, R.H. (2011) TDP-43-based animal models of neurodegeneration, new insights into ALS pathology and pathophysiology. *Neurodegener. Dis.*, **8**, 262–274.
6. Buratti, E. and Baralle, F.E. (2008) Multiple roles of TDP-43 in gene expression, splicing regulation, and human disease. *Front. Biosci.*, **13**, 867–878.
7. Buratti, E. and Baralle, F.E. (2011) TDP-43, New aspects of autoregulation mechanisms in RNA binding proteins and their connection with human disease. *FEBS J.*, **278**, 3530–3538.
8. Igaz, L.M., Kwong, L.K., Lee, E.B., Chen-Plotkin, A., Swanson, E., Unger, T., Malunda, J., Xu, Y., Winton, M.J., Trojanowski, J.Q. *et al.* (2011) Dysregulation of the ALS-associated gene TDP-43 leads to neuronal death and degeneration in mice. *J. Clin. Invest.*, **121**, 726–738.
9. Feiguin, F., Godena, V.K., Romano, G., D'Ambrogio, A., Klima, R. and Baralle, F.E. (2009) Depletion of TDP-43 affects Drosophila motoneurons terminal synapsis and locomotive behavior. *FEBS Lett.*, **583**, 1586–1592.
10. Fiesel, F.C., Voigt, A., Weber, S.S., Van den Haute, C., Waldenmaier, A., Görner, K., Walter, M., Anderson, M.L., Kern, J.V., Rasse, T.M. *et al.* (2010) Knockdown of transactive response DNA-binding protein (TDP-43) downregulates histone deacetylase 6. *EMBO J.*, **29**, 209–221.
11. Voigt, A., Herholz, D., Fiesel, F.C., Kaur, K., Müller, D., Karsten, P., Weber, S.S., Kahle, P.J., Marquardt, T. and Schulz, J.B. (2010) TDP-43-mediated neuron loss in vivo requires RNA-binding activity. *PLoS ONE*, **5**, e12247.
12. Sephton, C.F. *et al.* (2010) TDP-43 is a developmentally regulated protein essential for early embryonic development. *J. Biol. Chem.*, **285**, 6826–6834.
13. Wu, L.S. *et al.* (2010) TDP-43, a neuro-pathosignature factor, is essential for early mouse embryogenesis. *Genesis*, **48**, 56–62.
14. Lieschke, G.J. and Currie, P.D. (2007) Animal models of human disease, zebrafish swim into view. *Nat. Rev. Genet.*, **8**, 353–367.
15. Bandmann, O. and Burton, E.A. (2010) Genetic zebrafish models of neurodegenerative diseases. *Neurobiol. Dis.*, **40**, 58–65.
16. Ramesh, T., Lyon, A.N., Pineda, R.H., Wang, C., Janssen, P.M., Canan, B.D., Burghes, A.H. and Beattie, C.E. (2010) A genetic model of amyotrophic lateral sclerosis in zebrafish displays phenotypic hallmarks of motor neuron disease. *Dis. Model. Mech.*, **3**, 652–662.
17. Armstrong, G.A. and Drapeau, P. (2013) Calcium channel agonists protect against neuromuscular dysfunction in a genetic model of TDP-43 mutation in ALS. *J. Neurosci.*, **33**, 1741–1752.
18. Kabashi, E., Lin, L., Tradewell, M.L., Dion, P.A., Bercier, V., Bourgouin, P., Rochefort, D., Bel Hadj, S., Durham, H.D., Vande Velde, C. *et al.* (2010) Gain and loss of function of ALS-related mutations of TARDBP (TDP-43) cause motor deficits *in vivo*. *Hum. Mol. Genet.*, **19**, 671–683.
19. Robu, M.E., Larson, J.D., Nasevicius, A., Beiraghi, S., Brenner, C., Farber, S.A. and Ekker, S.C. (2007) p53 activation by knockdown technologies. *PLoS Genet.*, **3**, e78.
20. Kraemer, B.C., Schuck, T., Wheeler, J.M., Robinson, L.C., Trojanowski, J.Q., Lee, V.M. and Schellenberg, G.D. (2010) Loss of murine TDP-43 disrupts motor function and plays an essential role in embryogenesis. *Acta Neuropathol.*, **119**, 409–419.
21. Ayala, Y.M., Misteli, T. and Baralle, F.E. (2008) TDP-43 regulates retinoblastoma protein phosphorylation through the repression of cyclin-dependent kinase 6 expression. *Proc. Natl Acad. Sci. USA*, **105**, 3785–3789.
22. Sendtner, M. (2011) TDP-43, multiple targets, multiple disease mechanisms? *Nat. Neurosci.*, **14**, 403–405.
23. DeJesus-Hernandez, M., Mackenzie, I.R., Boeve, B.F., Boxer, A.L., Baker, M., Rutherford, N.J., Nicholson, A.M., Finch, N.A., Flynn, H., Adamson, J. *et al.* (2011) Expanded GGGGCC hexanucleotide repeat in noncoding region of C9ORF72 causes chromosome 9p-linked FTD and ALS. *Neuron*, **72**, 245–256.
24. Renton, A.E., Majounie, E., Waite, A., Simón-Sánchez, J., Rollinson, S., Gibbs, J.R., Schymick, J.C., Laaksovirta, H., van Swieten, J.C., Myllykangas, L. *et al.* (2011) A hexanucleotide repeat expansion in C9ORF72 is the cause of chromosome 9p21-linked ALS-FTD. *Neuron*, **72**, 257–268.
25. Cooper-Knock, J., Hewitt, C., Highley, J.R., Brockington, A., Milano, A., Man, S., Martindale, J., Hartley, J., Walsh, T., Gelsthorpe, C. *et al.* (2012) Clinico-pathological features in amyotrophic lateral sclerosis with expansions in C9ORF72. *Brain*, **135**, 751–764.
26. Buratti, E. and Baralle, F.E. (2010) The multiple roles of TDP-43 in pre-mRNA processing and gene expression regulation. *RNA Biol.*, **7**, 420–429.
27. Iguchi, Y., Katsuno, M., Niwa, J., Yamada, S., Sone, J., Waza, M., Adachi, H., Tanaka, F., Nagata, K., Arimura, N. *et al.* (2009) TDP-43 depletion induces neuronal cell damage through dysregulation of Rho family GTPases. *J. Biol. Chem.*, **284**, 22059–22066.
28. Gould, T.W., Buss, R.R., Vinsant, S., Prevette, D., Sun, W., Knudson, C.M., Milligan, C.E. and Oppenheim, R.W. (2006) Complete dissociation of motor neuron death from motor dysfunction by Bax deletion in a mouse model of ALS. *J. Neuroscience.*, **26**, 8774–8786.
29. McWhorter, M.L., Monani, U.R., Burghes, A.H. and Beattie, C.E. (2003) Knockdown of the survival motor neuron (Smn) protein in zebrafish causes defects in motor axon outgrowth and pathfinding. *J. Cell Biol.*, **162**, 919–931.
30. Murray, L.M., Talbot, K. and Gillingwater, T.H. (2010) Review, neuromuscular synaptic vulnerability in motor neuron disease, amyotrophic lateral sclerosis and spinal muscular atrophy. *Neuropathol. Appl. Neurobiol.*, **36**, 133–156.
31. Woods, I.G., Wilson, C., Friedlander, B., Chang, P., Reyes, D.K., Nix, R., Kelly, P.D., Chu, F., Postlethwait, J.H. and Talbot, W.S. (2005) The zebrafish gene map defines ancestral vertebrate chromosomes. *Genome Res.*, **15**, 1307–1314.
32. Chiang, P.M., Ling, J., Jeong, Y.H., Price, D.L., Aja, S.M. and Wong, P.C. (2010) Deletion of TDP-43 down-regulates Tbc1d1, a gene linked to obesity, and alters body fat metabolism. *Proc. Natl Acad. Sci. USA*, **107**, 16320–16324.
33. Avendaño-Vázquez, S.E., Dhir, A., Bembich, S., Buratti, E., Proudfoot , N. and Baralle, F.E. (2012) Autoregulation of TDP-43 mRNA levels involves interplay between transcription, splicing, and alternative polyA site selection. *Genes Dev.*, **26**, 1679–1684.
34. Ayala, Y.M., De Conti, L., Avendaño-Vázquez, S.E., Dhir, A., Romano, M., D'Ambrogio, A., Tollervey, J., Ule, J., Baralle, M., Buratti, E. *et al.* (2011) TDP-43 regulates its mRNA levels through a negative feedback loop. *EMBO J.*, **30**, 277–288.
35. Ayala, Y.M., Pagani, F. and Baralle, F.E. (2006) TDP43 depletion rescues aberrant CFTR exon 9 skipping. *FEBS Lett.*, **580**, 1339–1344.
36. Xu, Y.F., Gendron, T.F., Zhang, Y.J., Lin, W.L., D'Alton, S., Sheng, H., Casey, M.C., Tong, J., Knight, J., Yu, X. *et al.* (2010) Wild-type human TDP-43 expression causes TDP-43 phosphorylation, mitochondrial aggregation, motor deficits, and early mortality in transgenic mice. *J. Neurosci.*, **30**, 10851–10859.
37. Swarup, V., Phaneuf, D., Bareil, C., Robertson, J., Rouleau, G.A., Kriz, J. and Julien, J.P. (2011) Pathological hallmarks of amyotrophic lateral sclerosis/frontotemporal lobar degeneration in transgenic mice produced with TDP-43 genomic fragments. *Brain*, **134**, 2610–2626.
38. Xu, Y.-F., Gendron, T.F., Zhang, Y.-J., Lin, W.-L., D'Alton, S., Sheng, H., Casey, M.C., Tong, J., Knight, J., Yu, X. *et al.* (2010) Wild-type human TDP-43 expression causes TDP-43 phosphorylation, mitochondrial aggregation, motor deficits, and early mortality in transgenic mice. *J. Neurosci.*, **30**, 10851–10859.
39. Kawakami, K., Shima, A. and Kawakami, N. (2000) Identification of a functional transposase of the Tol2 element, an Ac-like element from the Japanese medaka fish, and its transposition in the zebrafish germ lineage. *Proc. Natl Acad. Sci. USA*, **97**, 11403–11408.
40. Beattie, C.E., Melancon, E. and Eisen, J.S. (2000) Mutations in the stumpy gene reveal intermediate targets for zebrafish motor axons. *Development*, **127**, 2653–2662.
41. Tang, R., Dodd, A., Lai, D., McNabb, W.C. and Love, D.R. (2007) Validation of zebrafish (Danio rerio) reference genes for quantitative real-time RT–PCR normalization. *Acta Biochim. Biophys. Sin (Shanghai).*, **39**, 384–390.